13th International Symposium on Particle Image Velocimetry – ISPIV 2019
Munich, Germany, July 22-24, 2019

Adjoint-based Data Assimilation for a Compressible Jet using PIV

Paul Schwarz*, **Mathias Lemke, Jörn Sesterhenn**

Institut für Strömungsmechanik und Technische Akustik, Technische Universität Berlin, Germany
*paul.schwarz@tnt.tu-berlin.de

Abstract

An adjoint-based data assimilation is used to adapt the boundary conditions of a numerical simulation to reproduce a specific experimental flow realization. The result is a full solution of the Navier-Stokes equations, ready for further analysis. The specific aim of this work is to analyze a subsonic jet flow.

1 Introduction

For a variety of engineering applications it is desirable to determine the pressure field in a flow. The corresponding information can be used, for example, to analyze and optimize the shape of bluff bodies, e.g. with respect to drag and lift. Several methods for pressure determination exist. Typical experimental techniques, like pressure transducer are impractical, e.g. there is not enough space for the sensors or the influence of the instruments lead to a disturbed flow field. This is why many recent methods are based on optical methods which are often restricted to velocity measurements, in particular particle image velocimetry (PIV). In conjunction with improved PIV techniques, such as Tomo-PIV (Elsinga et al., 2006) or Shake-The-Box (Schanz et al., 2013), other methods have been developed to determine the pressure from velocity measurement data, see (Blinde et al., 2016) for an overview.

This paper presents the application of an adjoint-based data assimilation framework for pressure determination in compressible flows, using PIV data. The overall idea is to adapt a numerical simulation towards experimental data. Once the numerical simulation matches the experimental data (e.g. velocities) in an optimal sense, unmeasured data, like pressure, can be obtained from the numerical solution. The method was reported in (Lemke et al., 2016) for compressible flows. A similar approach for incompressible flows is described in (Gronskis et al., 2013). In comparison with other approaches the method has the benefit to determine the full state of a flow, e.g. density and temperature.

In this work the method is employed to analyze a two-dimensional compressible jet flow. Planar PIV data are used as target data for the data assimilation. The boundary conditions of a numerical simulation are adapted until the numerical velocity field match the experimental data.

2 The Adjoint Approach

Consider the following minimization problem

$$\begin{aligned} \min_{q} \quad & J = \frac{1}{2}\int_{\Omega} \left(q - \tilde{C}^{-1}\left(C\left(q_{exp}\right)\right)\right)^2 \sigma(x,t)\mathrm{d}\Omega \\ \text{s.t.} \quad & \int_{\Omega} \left(N(q,f)\right)\mathrm{d}\Omega\,. \end{aligned} \tag{1}$$

The aim of the adjoint framework is to minimize the quadratic objective function J under the constraint, that the compressible Navier-Stokes equation ($N(q, f)$) are satisfied. By adaptation of a forcing f the system state q is modified in order to match the experimental state q_{exp}.
The term $\sigma(x,t)$ is a weight in space and time, $C(q)$ is the observer function (camera function) and $\tilde{C}^{-1}$ its approximative inverse (the PIV algorithm). We assume in this paper $\tilde{C}^{-1}(C(\cdot)) = I$.

Minimizing the objective function by testing random forcing values, in the sense of a parameter study, leads to prohibitive computational costs. However, the adjoint allows to significantly reduce the computational cost to determine an optimal f as it provides an efficient way to compute the required gradient information. The gradient is used in context of a standard steepest-descent method in order to minimize the objective or modify the system state respectivly.

For introducing the adjoint method different approaches are present in literature e.g. the Lagrange viewpoint or the duality formulation. The latter is presented here.

Consider the objective function

$$J = g^T q \tag{2}$$

defined as the product between a weighting g and the system state q. The system state is the solution of the governing equation

$$Aq = f. \tag{3}$$

Therein, A is the governing operator and f the forcing term on the right-hand side. As mentioned above it is expensive to compute the governing equation for multiple f to study the impact on the objective function. To reduce the computational effort the adjoint equation can be used

$$A^T q^* = g. \tag{4}$$

The structure is similar to equation (3) where q^* is the adjoint solution. Based on the adjoint equation a formulation is found which connect the objective function directly with the forcing term

$$J = g^T q = g^T A^{-1} A q = \left(g^T A^{-1}\right)(Aq) = \left(A^{-T} g\right)^T f = {q^*}^T f. \tag{5}$$

This allows to compute the objective function for different f by a cheap scalar product. Therefore, its only necessary to compute the adjoint solution. If the problem is non-linear the formulation must be linearized as follows:

$$\delta J = g^T \delta q = {q^*}^T \delta f. \tag{6}$$

A small change in the objective function is equivalent to the product between the adjoint solution and a small change in the forcing.

2.1 The adjoint Navier-Stokes equation

To introduce the adjoint method for partial differential equations, in particular compressible flows, the friction terms are neglected for brevity and only the Euler equations are considered

$$\partial_t \begin{pmatrix} \rho \\ \rho u_i \\ \frac{p}{\gamma-1} \end{pmatrix} + \partial_{x_i} \begin{pmatrix} \rho u_i \\ \rho u_i u_j + p\delta_{ij} \\ \frac{u_i p \gamma}{\gamma-1} \end{pmatrix} - u_i \partial_{x_i} \begin{pmatrix} 0 \\ 0 \\ p \end{pmatrix} = f. \tag{7}$$

Therein the density is denoted as ρ, the velocity as u_i and p as pressure, as expression for the inner energy. The adiabatic coefficient is denoted by γ. The summation convention for indices i and j applies. On the right-hand side f describe the forcing term to be adapted. The equation can be abbreviated in vector form as

$$\partial_t a + \partial_{x_i} b^i + C^i \partial_{x_i} c = f. \tag{8}$$

As discussed above, the equation must be linearized with respect to the actual system state $q = (\rho, u_i, p)^T$.

$$\partial_t \frac{\partial a_\alpha}{\partial q_\beta} \delta q_\beta + \partial_{x_i} \frac{\partial b_\alpha}{\partial q_\beta} \delta q_\beta + C^i \partial_{x_i} \delta q_\beta + \delta C^i \partial_{x_i} c_\beta = \delta f \tag{9}$$

The state $\delta q = (\delta\rho, \delta u_i, \delta p)^T$ corresponds to the solution of the linearized equations. Inspired by the Lagrangian approach a multiplier q^* is added to the integral objective also linearized. Per definition the implicit formulation of the linearized governing equation is equal to zero. Based on this, the adjoint solution can be derived. Here, $\mathrm{d}\Omega$ means the space-time measure.

$$\iint \delta J \,\mathrm{d}\Omega = \iint g^T \delta q \,\mathrm{d}\Omega - \iint q^{*^T} \underbrace{\left(\partial_t A \delta q + \partial_{x_i} B^i \delta q + C^i \partial_{x_i} \delta q + \delta C^i \partial_{x_i} - \delta f\right) \mathrm{d}\Omega}_{=0}. \tag{10}$$

Resorting and partial integration leads to a formulation for the objective function δJ which is independent of δq

$$\begin{aligned}\iint \delta J \mathrm{d}\Omega = \iint q^{*^T} \delta f \mathrm{d}\Omega + \iint \delta q^T \underbrace{\left(g + A^T \partial_t q^* + B^{i^T} \partial_{x_i} q^* + \partial_{x_i} C^{i^T} q^* - \tilde{C}^i \partial_{x_i} c\right)}_{I} \mathrm{d}\Omega \\ - \underbrace{\left[\int \delta q^T A^T q^* \mathrm{d}x_i\right]_{t=t_0}^{t=t_{end}}}_{II} - \underbrace{\left[\int \delta q^T B^{i^T} q^* \mathrm{d}t\right]_{x_i=x_{i,0}}^{x_i=L_i} - \left[\int \delta q^T C^{i^T} q^* \mathrm{d}t\right]_{x_i=x_{i,0}}^{x_i=L_i}}_{III}.\end{aligned} \tag{11}$$

Part (I) represents the adjoint equation. Part (II) and (III) contain information about the adjoint initial- and boundary conditions and also have to vanish.
In summary, the solution q^* of the adjoint equation

$$\partial_t q^* + A^{T^{-1}} B^{i^T} \partial_{x_i} q^* + A^{T^{-1}} C^{i^T} \partial_{x_i} q^* - A^{T^{-1}} \tilde{C}^i \partial_{x_i} q^* + A^{T^{-1}} g = 0 \tag{12}$$

leads to an efficient method to compute the change of the objective function.

$$\iint \delta J \mathrm{d}\Omega = \iint q^{*^T} \delta f \mathrm{d}\Omega. \tag{13}$$

Thus, the multiplier q^* can be interpreted as a gradient or sensitivity.

2.2 The adjoint algorithm

Starting with an initial guess f^0 the governing Navier-Stokes equations are solved. The computed system state is compared to the experimental data. Afterwards, the adjoint equations are solved backwards in time. The adjoint solution is used to compute the gradient $\nabla_f J$ which is used to update the actual forcing $f^{n+1} = f^n + \nabla_f J$. Starting with a new solution of the governing equations the whole loop is repeated until the direct solution and the measurement values match in an optimal sense.

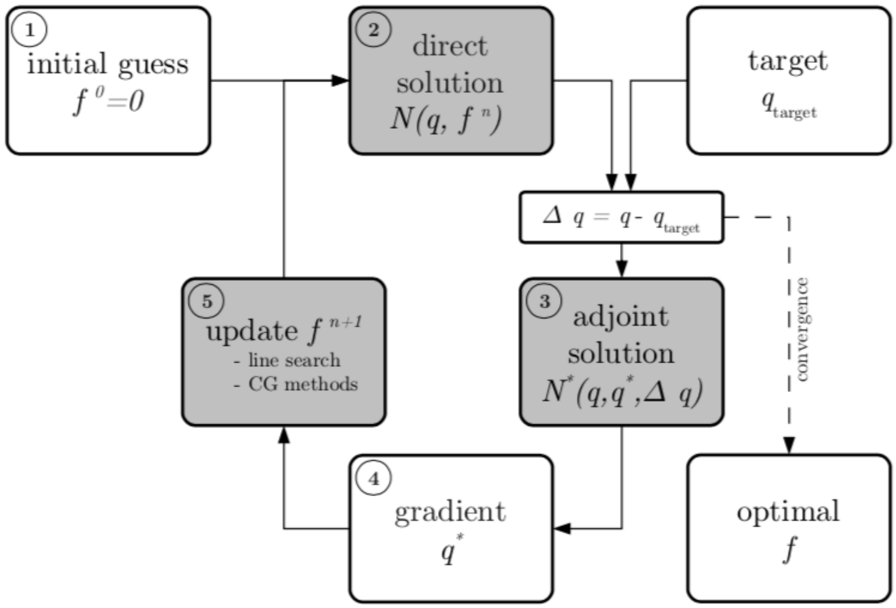

Figure 1: Illustration of the iterative data assimilation procedure using the adjoint approach.

3 Experimental setup

To demonstrate the applicability of the adjoint-based framework a suitable test setup created. Therefore, the windtunnel in Fig. 2 is used. A compressor with a tank of 3 m^3 at 10 bar is connected to control the flow. The flow direction in the sketch is from right to left. The windtunnel is constructed in a modular manner and consist of

1. the convergent nozzle
2. several distance modules
3. a shock-less diffusor
4. a grid module for homogenizing the flow by breaking up large flow pattern
5. a sintered module for smooth flow transition from a circular to the rectangular cross section.

Figure 2: Sketch of the modular experimental setup.

The total length of the convergent nozzle is 60.2 mm. The initial nozzle cross section is $168.5\,\text{mm} \times 50.8\,\text{mm}$ while the flow leaves the nozzle at the exit with a cross section of $168.5\,\text{mm} \times 11\,\text{mm}$ and a velocity up to $125\,\text{m/s}$, a corresponding Mach number of 0.29 Ma and a Reynolds number of $65,000$ Re. Therefore, the flow can be assumed slightly compressible. The aim is to generate a two-dimensional flow. The complete experimental set-up is shown in Fig. 3. To reduce secondary flow effects a wooden plate is mounted at the nozzle exit.

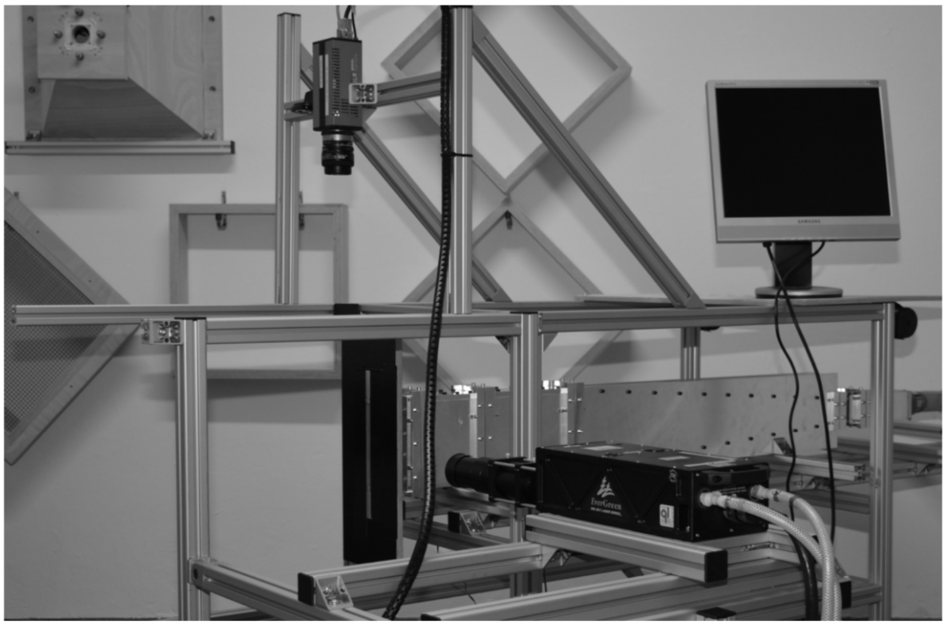

Figure 3: The experimental setup.

For observing the flow a standard planar two component (2D-2C) PIV system is used (PCO.2000 camera). The laser sheet is generated with a Evergreen 145 Laser from Quantel SA which is placed in the center of the nozzle exit. The region of interest is about $160\,\text{mm} \times 137\,\text{mm}$ resolved with $2.048\,\text{Px} \times 1.750\,\text{Px}$. The system is synchronized with a repetition rate of 7.5 Hz. The pulse distance for the double images is $7\,\mu$s. DEHS was used as seeding.

The velocity calculation was done with the Matlab tool PIVLAB (Thielicke and Stamhuis, 2014) based on the recorded PIV images.

4 Results

As explained before, the aim is to solve the minimization problem (2.1). For this purpose the adjoint framework computes and modifies the solution of the direct numerical simulation until it matches with the measured velocity fields. The simulation parameters are described in Tab. 1. On all sides of the computational domain sponges are added (Mani, 2012) which serves as forcing f. The solution is only evaluated at σ_x the inner region surrounded by the black line in Fig. 4.

In Fig. 4 the measured flow field from PIV and the calculated velocity field from the simulation are compared. The area inside the black line represent the assimilated field. Outside, the algorithm has the freedom to choose appropriate, unphysical values. It can be seen that the adjoint framework results in a solution which corresponds to the experimental values. The main properties of the flow are reconstructed. The calculated velocities are of the same order of magnitude as the input values.

Table 1: Simulation parameter

Parameter	Value	description
L_{x_1}	35 mm	Domain size in x_1
L_{x_2}	40 mm	Domain size in x_2
N_{x_1}	256	Resolution in x_1
N_{x_2}	256	Resolution in x_2
h_{x_1}	0.14 mm	Step size in x_1
h_{x_2}	0.16 mm	Step size in x_2
dt	4.17×10^{-7} s	Step size in time
nt	1500	Number of Timesteps
ρ_∞	$1.2040\,\mathrm{Kg/m^3}$	Initial density
P_∞	1×10^5 Pa	Initial pressure
T_∞	300 K	Initial temperatur

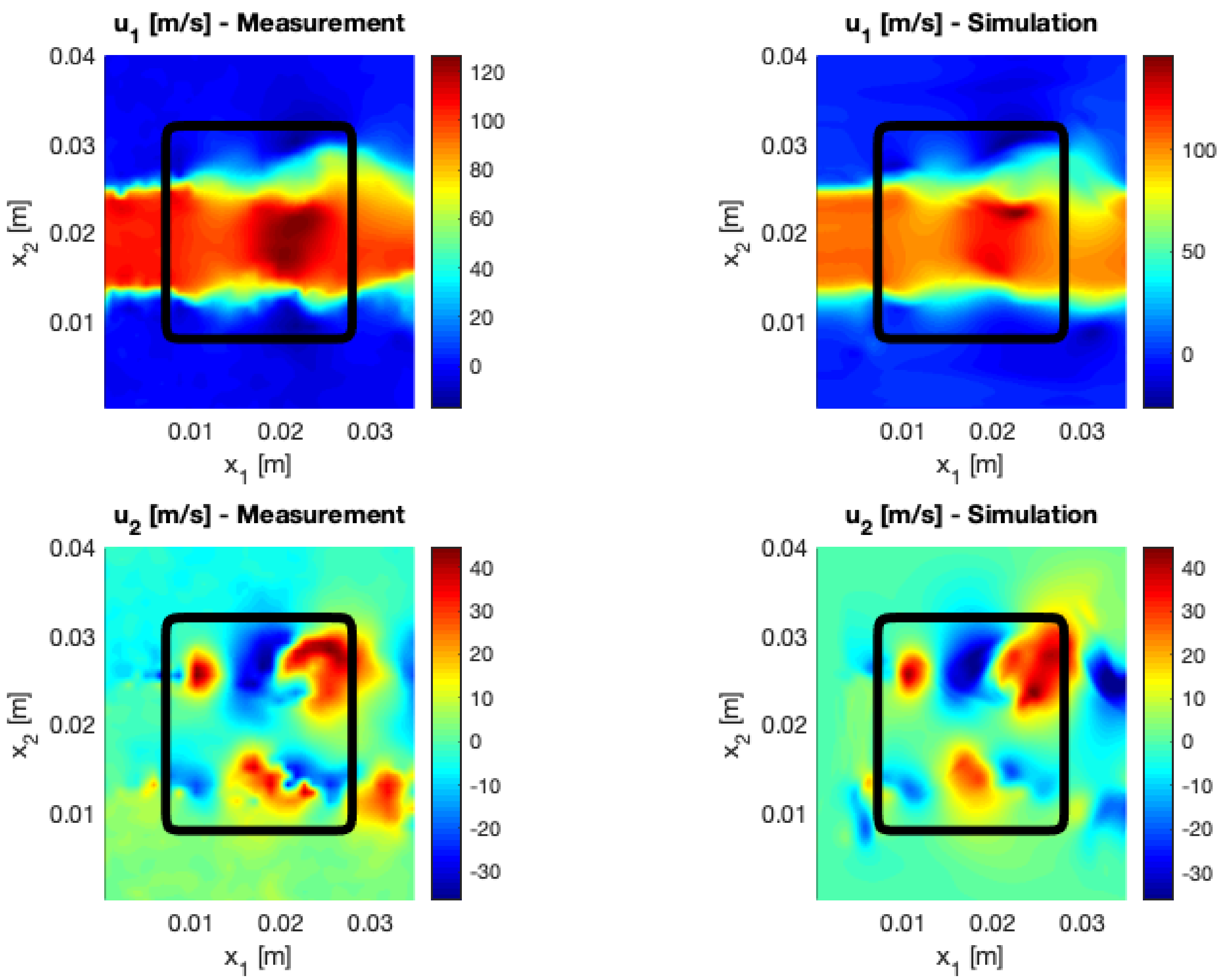

Figure 4: Comparison between the measurement velocity field (left) and the simulation results (right).

The graph in Fig. 5 shows the progress of the objective function within 180 iterations. The objective at the end is reduced by nearly one order of magnitude

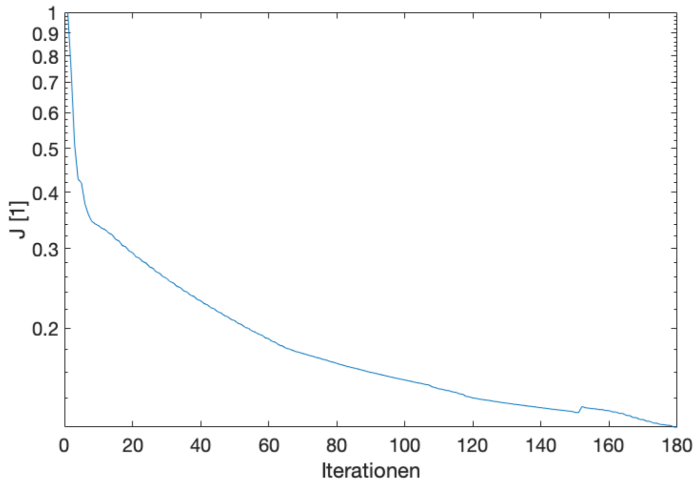

Figure 5: Progress of the the objective function.

5 Conclusion and Outlook

Previous works of the authors (Lemke and Sesterhenn, 2013), (Lemke, 2015), (Lemke et al., 2016) have shown the general possibility to determine pressure or even full state information from PIV images by using an adjoint data assimilation method.

The immediate next steps include the assimilation of a full, laminar Jet at low Reynolds number. Therefore, a vacuum chamber, see Fig. 6, was build, which allows to control the Reynolds number by changing the pressure in the facility. The inflow conditions can be changed by the outer channel 6a by means of different orifices. With different nozzles inside the chamber the jet structure can be influenced. In Fig 6c the actually installed 2D nozzle can be seen.

(a) The frontview with the outer channel.

(b) Sideview of the open chamber.

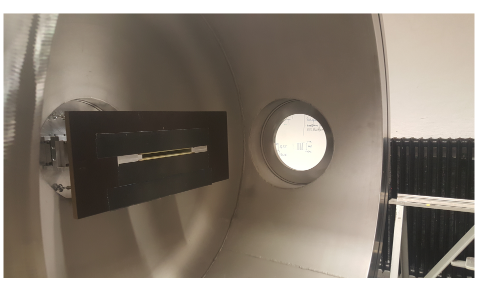

(c) The inner chamber with the discribed noozle.

(d) Sideview with the observation windows on the left, top, and bottom of the chamber.

Figure 6: The vaccum chamber for generating and observing flows at low Reynolds numbers.

References

Blinde P, Michaelis D, van Oudheusden B, Weiss P, de Kat R, Laskari A, Jeon J, David L, Schanz D, and Huhn F (2016) Comparative assessment of PIV-based pressure evaluation techniques applied to a transonic base flow. *18th International Symposium on the Application of Laser Imaging Techniques to Fluid Mechanics*

Elsinga GE, Scarano F, Wieneke B, and Van Oudheusden BW (2006) Tomographic particle image velocimetry. *Experiments in Fluids* 41:933–947

Gronskis A, Heitz D, and Mémin E (2013) Inflow and initial conditions for direct numerical simulation based on adjoint data assimilation. *Journal of Computational Physics* 242:480–497

Lemke M (2015) *Adjoint based data assimilation in compressible flows with application to pressure determination from PIV data*. Ph.D. thesis

Lemke M, Reiss J, Sesterhenn J, Lemke M, Reiss J, and Sesterhenn J (2016) Pressure Estimation from PIV like Data of Compressible Flows by Boundary Driven Adjoint Data Assimilation. *American Institute of Physics* 030017

Lemke M and Sesterhenn J (2013) Adjoint based pressure determination from PIV-data – Validation with synthetic PIV measurements –. *10th International Symposium on Particle Image Velocimetry* pages 1–10

Mani A (2012) Analysis and optimization of numerical sponge layers as a nonreflective boundary treatment. *Journal of Computational Physics* 231:704–716

Schanz D, Schröder A, Gesemann S, Michaelis D, and Wieneke B (2013) ‘ Shake The Box ’: A highly efficient and accurate Tomographic Particle Tracking Velocimetry (TOMO-PTV) method using prediction of particle positions. *10th International Symposium on Particle Image Velocimetry - PIV13 Delft, The Netherlands, July 1-3* pages 1–13

Thielicke W and Stamhuis EJ (2014) PIVlab – Towards User-friendly, Affordable and Accurate Digital Particle Image Velocimetry in MATLAB. *Journal of Open Research Software 2(1):e30*